

Understanding hierarchical protein evolution from first principles

Nikolay V. Dokholyan* and Eugene I. Shakhnovich†

Department of Chemistry, Harvard University, 12 Oxford Street, Cambridge, MA 02138, USA

We propose a model that explains the hierarchical organization of proteins in fold families. The model, which is based on the evolutionary selection of proteins by their native state stability, reproduces patterns of amino acids conserved across protein families. Due to its dynamic nature, the model sheds light on the evolutionary time scales. By studying the relaxation of the correlation function between consecutive mutations at a given position in proteins, we observe separation of the evolutionary time scales: at the short time intervals families of proteins with similar sequences and structures are formed, while at long time intervals the families of structurally similar proteins that have low sequence similarity are formed. We discuss the evolutionary implications of our model. We provide a “profile” solution to our model and find agreement between predicted patterns of conserved amino acids and those actually observed in nature.

Key words: protein evolution, Z -score model, profile solution

I. INTRODUCTION

Understanding protein evolution still remains a major challenge in molecular biology [1–13]. While the mechanisms of mutations in DNA sequences that code for proteins are known [14], the selective fixation of these mutations in proteins is far from clear. Mutations occurring in DNA are directly governed by physical-chemical processes and their fixation is subject to cellular repair mechanisms being able to preserve nucleotide(s) from modifications. Selection by evolution is much softer in DNA than in proteins due to a stronger inter-dependence of the protein structure, function and kinetic properties than that of DNA. Since mutations may drastically alter the physical, chemical, and biological properties of proteins, evolution exerts pressure to preserve those amino acids that play an important role in the folding kinetics, functionality and stability of proteins. Our goal is to understand evolution from the statistical mechanics perspective.

There are several principal facts observed in proteins: *(i)* a protein sequence folds into a unique three-dimensional structure (there might be exceptions, e.g. prions); *(ii)* protein sequences are *selected*, i.e. a randomly chosen polypeptide most likely aggregates in solution without forming any definite three-dimensional structure; *(iii)* proteins taken from various species and having sequence identity, ID , at least $ID = 25 - 30\%$ have similar three-dimensional structures (*native state*) [12,15–21] and are said to belong to the same fold family; *(iv)* some pairs of proteins sharing the same fold have sequence similarity as low as expected for random sequences $ID \sim 8 - 9\%$ [9,22,23]; *(v)* within the same fold family, protein sequences have only 3 – 4% “anchored” amino acids [9]. A set of proteins that have at least 25% sequence similarity and are structurally similar are called homologs. A set of structurally similar proteins that may have less than 25% sequence similarity is called a group of structurally homologous proteins or analogs. Analogs include several families of homologs and generally constitute a larger set of proteins than homologs. Known homologs and analogs are collected in the HSSP [19] and FSSP [22] databases respectively and are the subject of our study.

Here we propose a model of evolution (*Z-score model*) that, based on facts *(i)* and *(ii)*, attempts to reproduce the rest of remaining principal observations *(iii) – (v)* described above. The Z -score model is based on the design of a set of structurally identical sequences by the Z -score minimization [24–26]. The idea is to find the similarities in the sequences of such a set and to recover those residues that are conserved across this set. The protein folding theory [27,28] suggests that Z -score minimization is equivalent to maximizing the energy gap between misfolded or unfolded conformations and the native state of a protein. It has been pointed out that such maximization results in stable and fast-folding proteins [24,29]. Thus, by designing sequences that have the same fold, we attempt to mimic evolution in diversifying protein sequences for the same fold family. In addition, the Z -score model is a dynamical model, i.e. there is an implicit time scale that allows one to follow the evolution of sequences during the design procedure. The model is discussed in detail in Sec. II and a profile approximation to this model is outlined in Sec. III. In Sec. IV we show that our view of evolution proposed below is consistent with the implications of the proposed model. Next we discuss our scenario of protein evolution.

*Email: dokh@wild.harvard.edu

†Email: eugene@belok.harvard.edu

We conjecture that hierarchical organization of structurally similar proteins may be the result of the separation of the evolutionary time scales, shown schematically on Fig. 1. On a time scale τ_o , a set of mutations occur that do not affect those amino acids that play thermodynamical, kinetical and/or functional roles. As a result, there is little variation in sequences at the important sites of proteins. If a mutation occurs at the thermodynamically, kinetically and/or functionally important sites, it usually substitutes amino acids with close physical properties so that core, nucleus and/or functional site are not disrupted and the protein folds into its family fold, is stable in this fold, and its function is preserved. At this time scale, a family of homologs is born.

Rarely, at time scale τ , correlated mutations occur [30–32] that modify *several* amino acids at the core, nucleus and/or functional site, so that the stability and kinetics of proteins are not altered. Such a set of mutations can drastically modify the sequence of the protein. However, within the time scale τ_o , a family of homologs is born within which there is conservation of (already new) amino acids in the specific (important) sites of homologous proteins. Although there are alternations in the specific sites of the proteins at the time scale τ , these sites are more preserved than the rest of the sequence. The proposed view of protein evolution is consistent with the observations of hierarchical organization of structurally similar proteins in families of homologs. Sets of families of homologs are organized, in turn, in super-families of analogs.

II. Z-SCORE MODEL

We start with a random protein amino acid sequence and perform a Monte Carlo search for the mutation that energetically favors interactions in such a sequence. The Monte Carlo design algorithm is based on the minimization of the so-called Z -score, defined as

$$Z = \frac{E_{NS} - \langle E \rangle}{\sigma(E)}, \quad (1)$$

which corresponds to the minimization of the energy gap between the native state, E_{NS} , of the selected sequence and the average energy, $\langle E \rangle$, of structurally unrelated conformations (decoys) [33–35]. $\sigma(E)$ is the standard deviation of energies of all decoys (see Fig. 2).

Since Z -score minimization is equivalent to maximizing the energy gap between misfolded or unfolded conformations and the native state of the protein [27,28,33], such maximization results in stable and fast-folding proteins. The energy gap must be “significant”, meaning that E_{NS} must deviate from $\langle E \rangle$ by many standard deviations σ : $E_{NS} \ll \langle E \rangle - \sigma$. Many researchers have pointed out (see, e. g., review [29]) that minimization of the Z -score corresponds to the stabilization of the protein in its native state.

The design proceeds as follows: (i) we select an amino acid σ_i at a random position $1 \leq i \leq N$; (ii) we substitute this amino acid by σ'_i with probability p ,

$$p = \begin{cases} 1, & \text{if } \delta Z < 0 \\ \exp(-\delta Z/T_{des}), & \text{if } \delta Z > 0, \end{cases} \quad (2)$$

where $\delta Z = Z(\sigma'_i) - Z(\sigma)$ is the difference between the Z -scores of the mutated and the original proteins. We design each of $N_s = 100$ sequences by running the simulations for N_m Monte Carlo steps at some design temperature, T_{des} .

Computation of $\langle E \rangle$ and $\sigma(E)$ is straightforward:

$$\langle E \rangle = \frac{1}{2} \sum_{i \neq j} U(\sigma_i, \sigma_j) f_{ij}, \quad (3)$$

and

$$\sigma^2(E) = \langle (E - \langle E \rangle)^2 \rangle = \frac{1}{2} \sum_{i \neq j} f_{ij} (1 - f_{ij}) U^2(\sigma_i, \sigma_j) + \mathcal{O}(f_{ij}^2). \quad (4)$$

where f_{ij} is the frequency of a contact between monomers i and j in a set of decoys, i. e.

$$f_{ij} = \langle \Delta_{ij} \rangle. \quad (5)$$

We estimate frequencies of contacts by making two assumptions about the set of decoys: (1) the distribution, $P(\ell = |i - j|; i, j)$ of the contact distances, $\ell = |i - j|$, between various amino acids at the positions i and j is universal

among globular proteins; and (2) the actual frequency of contacts between various amino acids, i and j , is only a function of the absolute value of the length of contacts, $|i - j|$, and is equal to the distribution of the contact lengths, i. e.

$$f_{ij} = f_{|i-j|} = f(\ell). \quad (6)$$

The distribution $P(\ell)$ is then

$$P(\ell) = \frac{f(\ell)}{\sum_{\ell=1}^N f(\ell)}. \quad (7)$$

Both assumptions, (1) and (2), are motivated by the fact that the variety of protein structures known to date samples adequately the conformational space of proteins under study and the variety is large enough that all the information about the secondary structure peculiarities of individual proteins are averaged out.

In order to estimate frequencies, f_{ij} , according to Eq. (7) we compute the distribution of contacts of length $\ell = |i - j|$ in the ensemble of approximately 10^3 representative globular proteins in Protein Data Bank (PDB) [36,37]. The distribution, shown in Fig. 3, is obtained using C_β -representation of proteins. The contacts are defined by Eq. (20).

The estimation of contact frequencies f_{ij} is one of the key ingredients to protein design. An alternative approach based on sampling of homopolymer conformations appears to be less efficient, so we omit it in the present study. Nevertheless, due to its importance and possible potential for other studies, we discuss this approach in Appendix A.

After we obtain N_s number of designed sequences, we compute the probability of an amino acid σ_k to be in k th position, $P_Z(\sigma_k)$, as the frequency of occurrence of this amino acid,

$$P_Z(\sigma_k) = N(\sigma_k)/N_s, \quad (8)$$

where $N(\sigma_k)$ is the total number of occurrences of an amino acid σ_k at the position k . Next, using Eq. (22) we compute the sequence entropy, $S_Z(k)$.

III. PROFILE SOLUTION

We develop a profile solution to the Z -score model that provides a rationale for conservatism patterns caused by selection for stability. Our solution is of *equilibrium* evolution that maintains stability and other properties achieved at an earlier, prebiotic stage. To this end we propose that stability selection accepts only those mutations that keep energy of the native protein, E , below a certain threshold E_c necessary to maintain an energy gap [6,24,38,39]. The requirement to maintain an energy threshold for the viable sequences makes the equilibrium ensemble of sequences analogous to a microcanonical ensemble. In analogy with statistical mechanics, a more convenient and realistic description of the sequence ensemble is a canonical ensemble, whereby strict requirements on energy of the native state is replaced by a “soft” evolutionary pressure that allows energy fluctuations from sequence to sequence but makes sequences with high energy in the native state unlikely. In the canonical ensemble of sequences, the probability of finding a particular sequence, $\{\sigma\}$, in the ensemble follows the Boltzmann distribution [6,24,38,40]

$$P(\{\sigma\}) = \frac{\exp(-E\{\sigma\}/T)}{Z}, \quad (9)$$

where T is the effective temperature of the canonical ensemble of sequences that serves as a measure of evolutionary pressure and $Z = \sum_{\{\sigma\}} \exp(-E\{\sigma\}/T)$ is the partition function taken in sequence space.

Next, we apply a profile approximation that replaces all multiparticle interactions between amino acids with interaction of each amino acid with an effective field Φ acting on this amino acid from the rest of the protein, so that each amino acid experiences the exact field of its neighbors. This approximation presents $P(\{\sigma\})$ in a multiplicative form as $\prod_{k=1}^N p(\sigma_k)$ of probabilities to find an amino acid σ at position k [41]. $p(\sigma_k)$ also obeys Boltzmann statistics

$$p(\sigma_k) = \frac{\exp(-\Phi(\sigma_k)/T)}{\sum_{\sigma} \exp(-\Phi(\sigma_k)/T)}. \quad (10)$$

The profile potential $\Phi(\sigma_k)$ is the effective potential energy between amino acid σ_k and all amino acids interacting with it, i. e.

$$\Phi(\sigma_k) = \sum_{i \neq k}^N U(\sigma_k, \sigma_i) \Delta_{ki}. \quad (11)$$

The potential Φ is similar in spirit to the protein profile introduced by Bowie et al. [42] to identify protein sequences that fold into a specific 3D structure.

For each member, m , of the fold family (FSSP database [22]) presented in Fig. 1, we compute the profile probability, $p_m(\sigma_k)$, using Eq. (10). This probability, $p_m(\sigma_k)$, for each fold family member corresponds to the frequency of amino acids, σ_k , at positions, k , for a given family of homologs. Then, we compute the average profile probability over all members of the fold family,

$$p_P(\sigma_k) = \frac{1}{N_s} \sum_{m=1}^{N_s} p_m(\sigma_k). \quad (12)$$

This quantity corresponds to the $P_{acr}(\sigma_k)$ presented in [30]. Eqs. (10) — (12), along with the properly selected energy function, U , make it possible to predict probabilities of all amino acid types and sequence entropy $S_P(k)$ at each position k

$$S_P(k) = - \sum_{\sigma} p_P(\sigma_k) \ln p_P(\sigma_k) \quad (13)$$

from the native structure of a protein. The summation is taken over all possible values of σ .

If stability selection is a factor in the evolution of proteins and our model captures it, then we should observe a correlation between the predicted profile based sequence entropies, $S_P(k)$, and actual sequence entropies $S_{acr}(k)$ in real proteins. Thus, the question is: “Can we find such T , so that the predicted conservatism profile $S_P(k)$ matches the real one $S_{acr}(k)$?”

By varying the values of the temperature T in the range $0.1 \leq T \leq 4.0$, we minimize the distance, $D^2 \equiv \sum_{k=1}^N (S_P(k) - S_{acr}(k))^2$, between the predicted and observed conservatism profiles. We exclude from this sum such positions in structurally aligned sequences that have more than 50% gaps in the structural (FSSP) alignment. We denote by T_{sel} the temperature that minimizes D .

The proposed profile solution has a dual role. On one hand, it allows us to understand the selective temperature scale, T_{sel} , which is the measure of evolutionary optimization. On the other hand, the correlation coefficient between $S_P(k)$ and $S_{acr}(k)$ does not vary strongly in the range of T_{sel} from 0.19 to 0.34, thus, allowing one to use the effective temperature of $T_{sel} = 0.25$ to predict the actual conservatism profiles of proteins (see Table I).

IV. RESULTS AND DISCUSSION

We study five folds: Immunoglobulin fold (Ig), Oligonucleotide-binding fold (OB), Rossmann fold (R), α/β -plait (α/β -P), and TIM-barrel fold (TIM). The three-dimensional structures of the representative proteins of these five folds are shown in Fig. 4: (a) Tenascin (Third Fibronectin Type III Repeat), pdb:1TEN; (b) Major Cold Shock Protein 7.4 (Cspa (Cs 7.4)) of *Escherichia Coli*, pdb:1MJC; (c) chemotactic protein CheY, pdb:3CHY; (d) Acyl-Phosphatase (Common Type) From Bovine Testis, pdb:2ACY; (e) Endo-Beta-N-Acetylglucosaminidase F1, pdb:2EBN. We compute the correlation coefficient [43] between values of $S_P(k)$, obtained at T_{sel} , and $S_{acr}(k)$ for all five folds. The results are summarized in Table I. The plots of $S_P(k)$ and $S_{acr}(k)$ versus k , as well as their scatter plots, are shown in Figs. 13–17.

A. Z-score model

We find that correlation between $S_Z(k)$ and $S_{acr}(k)$ strongly depends on the number of mutations, N_m , we introduce during design of a protein. This fact is in accord with our view (see Fig. 1) of protein evolution. On a short time scale, $\tau_o \sim 10^2$ Monte Carlo steps, mutations rarely alter amino acids with specific important properties such as participation in stabilization of proteins and/or in the nucleation processes in folding kinetics of proteins. These mutations diversify the family, m , of homologs, \mathcal{M}_h^m . On a larger scale, $\tau \gg \tau_o$, correlated mutations [30–32] modify core and/or nucleus site(s) of the proteins without compromising their stability, folding rates and function(s). Thus, at the time scale τ evolution moves from one family of homologs to another, diversifying the underlying family of

analogs, $\mathcal{M}_a, \bigcup_m \mathcal{M}_h^m \subseteq \mathcal{M}_a$. The ensemble of analogs is still much smaller than the ensemble, \mathcal{M}_o , of all possible sequences ($\mathcal{M}_a \subseteq \mathcal{M}_o$), which is of the size 6^N (in a 6-letter alphabet) — for $N = 100$ residue protein this number is of the order of 10^{78} . These results are in agreement with the theoretical predictions [3,27,29,44–46] that there is a large number (of the order $e^{1.9N}$ [29]) of fast folding sequences with a given native structure and pronounced stability gaps $\Delta = E_{NS} - \langle E \rangle$.

It is important that for the small number of mutations we find correlation between entropies of the designed sequence, $S_Z(k)$, and the empirically observed one, $S_{acr}(k)$. This correlation depends on the input random number, indicating that the selected sequences constitute a family of homologs, \mathcal{M}_h^m , that is closer or more distant to an original sequence family of homologs, \mathcal{M}_h^o (both \mathcal{M}_h^m and \mathcal{M}_h^o belong to a given family of analogs, \mathcal{M}_a). Here we present the results for the selected ensembles of the designed sequences, \mathcal{M}_h^m , after being optimized during N_m mutations. More important than the correlation between $S_Z(k)$ and $S_{acr}(k)$, we find that the profiles of $S_Z(k)$ and $S_{acr}(k)$ are in visible concert with each other.

The temperature dependence of the Z -score exhibits a sharp transition at $T = T_c \approx 0.25$ (Fig. 5) for all studied proteins. Above T_c , protein design results in unstable sequences, while at temperatures much lower than T_c many of the residues “freeze” in their original states. Thus, we select T_c as our design temperature.

B. Degree of divergence of sequences

To assess the degree of similarity or divergence of sequences in the course of Z -score design at various time scales, we compute the distribution of hamming distances at these time scales. The hamming distance, $Hd(\{\sigma\}^{(1)}, \{\sigma\}^{(2)})$, between two sequences, $\{\sigma\}^{(1)}$ and $\{\sigma\}^{(2)}$, is defined as the number of distinct amino acids at equal positions in these two sequences divided by the length of the sequences, N :

$$Hd(\{\sigma\}^{(1)}, \{\sigma\}^{(2)}) = \frac{1}{N} \sum_{i=1}^N \left[1 - \delta(\sigma_k^{(1)} - \sigma_k^{(2)}) \right]. \quad (14)$$

Hamming distance has a simple interpretation — it is the degree of divergence between two sequences: when Hd is equal to 1, the sequences have no amino acids in common, when Hd is equal to 0, the sequences are exactly the same.

We compute the distribution of hamming distances between all designed sequences for two design times (a) $t_d = 10^3 \gg \tau_o$ (Fig. 6(a)) and (b) $t_d = 10^2 \sim \tau_o$ Monte Carlo steps (Fig. 6(b)), where τ_o is a characteristic time scale. We use 1MJC family of homologs (OB fold) as an example throughout this subsection. We also performed similar analysis with other folds and the results are qualitatively the same (not shown).

In the computation of the distribution in case (b) we omit all sequences with sequence similarity less than $ID = 55\%$ to mimic sequence collection in the HSSP database. This threshold sequence similarity, ID , is chosen so that the hamming distance distribution derived from the actual sequences in the HSSP database (Fig. 6(d)) is similar to ours. Given that we use a six-letter alphabet, the correspondence between ID used in HSSP and our ID is not well defined. Because in (b) we select only sequences with minimal threshold similarity, ID , there are no events with $Hd > 0.55$ in Fig. 6(b). In addition, the events with low $Hd \rightarrow 0$ are overrepresented in our simulations since we do not account for additional pressure due to function or kinetics that exists in real protein sequences. Therefore, the distribution in our simulations (Fig. 6(b)) has a more pronounced tail $Hd \rightarrow 0$ than that in real proteins (Fig. 6(d)).

At the long time scales (a) we find that most of the sequences are divergent from each other with average $\langle Hd \rangle \approx 0.7$. We observe the same result by computing the distribution of the hamming distances between all analogs belonging to the OB fold family present in the FSSP database (Fig. 6(c)). The only difference between simulated (Fig. 6(a)) and observed (Fig. 6(c)) distributions of hamming distances is the tail present in the simulated distribution corresponding to the sequences with a significant degree of similarity. This tail is due to the fact that we compare all sequence with all sequences, thus, effectively including similar sequences in our histogram. In the FSSP database, on the other hand, only distant sequences are present so that the tail corresponding to the close sequences in Fig. 6(c) is absent.

The distributions of hamming distances in protein families are in qualitative agreement with those observed in simulations and with our picture of hierarchical protein evolution. At short time scales sequences are not strongly separated from each other forming families of homologs, while at long time scales, a family of analogs is formed, comprised of strongly separated sequences but structurally similar proteins.

C. Determination of the family formation time scale

To quantify our observation of evolutionary time scales separation, we compute the relaxation times of the correlation function (at each protein position, k) in the course of Z -score design defined as

$$C_k(\tau) = \frac{1}{t_d N_s} \sum_{\alpha=1}^{N_s} \int_0^{t_d} \chi_k^{(\alpha)}(t, \tau) dt = \langle \langle \chi_k(\tau) \rangle \rangle_{t_d, N_s}, \quad (15)$$

where $\langle \langle \dots \rangle \rangle_{t_d, N_s}$ denotes average over simulation design time, t_d , and the number, N_s , of initial sequences. $\chi_k^{(\alpha)}(t, \tau)$ is a boolean indicator of whether an amino acid $\sigma_k(t + \tau)$ at position k at time $t + \tau$ is the same as the amino acid at time $\sigma_k(t)$ at the same position at time t :

$$\chi_k^{(\alpha)}(t, \tau) = \begin{cases} 1, & \sigma_k(t) = \sigma_k(t + \tau) \\ 0, & \sigma_k(t) \neq \sigma_k(t + \tau). \end{cases} \quad (16)$$

$C_k(\tau)$ measures the probability that a mutation does not occur at the position k in time τ . This function for most equilibrium systems decays exponentially,

$$C(\tau) \sim \exp(-\tau/\tau_o), \quad (17)$$

where τ_o is the relaxation time that is the average mutation time between subsequent mutations.

We also find that the correlation function computed for $N_s = 10^3$ and for $t_d = 10^3$ decays exponentially (see Fig 7) and relaxation times τ_o depend strongly on the positions of the amino acids under consideration. For example, the relaxation of the correlation functions for positions 1 (Ser in 1MJC) and 31 (Val) in 1MJC design vary by almost a factor of two: $\tau_o(\text{Ser1}) = 143$ and $\tau_o(\text{Val31}) = 387$ Monte Carlo steps. The fact that $\tau_o(\text{Ser1})$ is more than two times larger than $\tau_o(\text{Val31})$ indicates that Ser1 is likely to mutate more than twice in the time-span of a single Val31 mutation.

In addition, the distribution of the relaxation times (see Fig. 6) exhibits a pronounced peak at $\tau_o = 170$ Monte Carlo steps, indicating that for most protein positions relaxation occurs with this typical relaxation time. The relaxation times found from the correlation function analysis are in agreement with our observations in Secs. IV A and IV B. The long non-gaussian tail in the histogram of the relaxation times also suggests the presence of the conserved positions. In fact, this tail, composed of the conserved positions, strongly deviates from the rest of the distribution, which is well approximated by a Gaussian distribution.

D. Rates of amino acid substitutions and conservatism

A number of authors suggested [47–50] that study of the conserved amino acids in families of structurally similar proteins can shed light on the functionally, kinetically and thermodynamically important amino acids in proteins. The basic belief behind the majority of such studies is that evolution optimizes, to a certain extent, the properties of proteins so that they become more stable and have better folding and functional properties. Here we use the “optimization” hypothesis of molecular evolution to understand the universe of protein sequences by implication of molecular evolution. The link between conserved amino acids and their role in proteins has been widely studied [49,51–55].

A recent study of Mirny and Shakhnovich [30] identified the presence of universally conserved amino acids across the families of proteins sharing the same fold. These conserved residues have been linked to protein stability, kinetic properties or function. Various experiments [51,56–65] have identified some of the conserved residues to have predicted specific roles.

Direct evidence of the relationship between conservatism and the physical properties of amino acids can be accessed by calculating the rates of amino acid substitutions in the course of the Z -score design. By comparing mutational rates at various positions of the proteins, we attempt to reconstruct the conservatism of these positions across the family of analogous proteins. Starting with the sequence of a representative protein of a given fold we perform Z -score design for $t_d = 10^8$ Monte Carlo steps. The substitution rates are defined as

$$R(k) \equiv \frac{N_m(k)}{\hat{t}_d} = \frac{N}{t_d} \sum_{t=1}^{t_d} [1 - \delta(\sigma_k(t) - \sigma_k(t-1))], \quad (18)$$

where $N_m(k)$ is the number of mutations that occurred at the position k , $\delta(x)$ is a Kronecker function, equal to 1 if $x = 0$ and 0 otherwise, $\sigma_k(t)$ is an amino acid σ at the position k at time t , and $\hat{t}_d = t_d/N$ is the average number of attempted mutations per position in a protein. Thus, $R(k)$ from the Eq. (18) is inversely proportional to the average time between subsequent substitutions of amino acids at the position k ; the lower the $R(k)$ the longer the amino acid at the position k remains unchanged and, therefore, the more conservative is this position in the course of design.

We find that the rates of substitutions, $R(k)$, correlate with the conservatism patterns, S_{acr} (see Figs. 8 – 12). Since there is no obvious relation between $R(k)$ and S_{acr} , and, moreover, there is no reason to assume linear relation between these quantities, the linear regression has only an illustrative meaning of the correlations observed between $R(k)$ and S_{acr} (see Figs. 8 – 12(b) and Table I). Despite the likely lack of linear relation between the rates and the entropy, the correlation observed based on the assumption of linear dependence between $R(k)$ and S_{acr} is feasible.

The computation of mutational rates, $R(k)$, does not involve the tuning of any parameters. We can choose any non-zero temperature, given that the total number of Monte Carlo steps, t_d , in the course of design is large enough to obtain statistically significant values of $R(k)$. We also find that at $T_{des} = 0.25$ the data for $R(k)$ is identical after 10^7 Monte Carlo steps to that after 10^8 Monte Carlo steps, so the values of $R(k)$ are statistically significant.

Interestingly, the fastest rates are at most two times faster than the slowest rates. Such variability of rates might be due to the variability in physical properties of amino acids. It has been shown [66] that there are only two principal eigenvalues of Miyazawa-Jernigan energy matrix [67,68] and the remaining eigenvalues are close to each other. Such a “degeneracy” in eigenvalues accounts for the similarities in physical properties of amino acids.

Another possible reason for such a wide range of rate variability is the absence of the side chains in our model. The side chains are an additional factor that slow down the rates because of the frustrations caused by the multiple side chain conformations [69] and, possibly, increase the range of rate variability. Despite all the artifacts of our model, the correlation between $R(k)$ and S_{acr} is significant, which indicates that the model does qualitatively capture the evolutionary selection of proteins.

E. Profile solution

The correlation between $S_P(k)$ and $S_{acr}(k)$ is remarkable for all five folds and indicates that our profile approximation is able to select the conserved amino acids in protein fold families and properly describe the formation of families on the short time scales (Table I). It is fully expected that the correlation coefficient is smaller than 1. The reason for this is that computation of $S_P(k)$ takes into account evolutionary selection for stability only and it does not take into account possible additional pressure to optimize kinetic or functional properties.

The additional evolutionary pressure due to the kinetic or functional importance of amino acids results in pronounced deviations of S_P from S_{acr} for a few amino acids that may be kinetically or functionally important. A number of amino acids whose conservatism is much greater than predicted by our model form a group of “outliers” from otherwise very close correspondence between S_P and S_{acr} . To demonstrate that some of those amino acids are important for folding kinetics and, as such, they can be under additional evolutionary pressure, we color data points on the S_P versus S_{acr} scatter plot according to the range of ϕ -values [70] that the corresponding amino acids fall into. The thermodynamic and kinetic roles of individual amino acids were studied extensively (i) by Hamill et al. [71] for the TNfn3 (1TEN) protein, (ii) by López-Hernández and Serrano [58] for the chemotactic protein (CheY, pdb:3CHY), and (iii) by Chiti et al. [72] for muscle acylphosphatase (AcP, pdb:2ACY).

We use the ϕ -values for individual amino acids obtained in [58,71]. We observe that (i) for TNfn3 protein most of the points on Fig. 13(b) that belong to the outlier group have ϕ -values ranging from 0.2 to 1; (ii) for CheY protein most of the points (for which ϕ -values are known) on Fig. 15(b) that belong to the outlier have ϕ -values ranging from 0.3 to 1; and (iii) for AcP protein, one nucleic amino acid, Tyr11, is strongly conserved, more than predicted by the profile solution, while the second amino acid, Pro54, belonging to the nucleus [72] does not appear to be conserved. The third nucleus amino acid, Phe94, in AcP protein is excluded from our analysis due to the lack of data at position 94. The discrepancy of the Pro54 conservatism and its kinetic role may be attributed to the poor statistical significance of $S_{acr}(k)$ calculation at this position. Figs. 13(b), 15(b), and 16(b) demonstrate that the presence of additional evolutionary pressure due to the kinetic importance of amino acids results in stronger conservatism of specific positions than predicted by profile solution.

It has been conjectured (see e.g. [9]) that on average only 3 – 4% of residues are “anchor residues”, i.e. those that are more significantly conserved than the rest of the residues. In fact, this observation is supported by the $S_{acr}(k)$ profile of the sequences and their profile estimates $S_P(k)$ (see Figs. 13(a) – 17(a)). These 3 – 4% of “anchor residues” are the principal “gates” to the structure/kinetics of a given family of proteins. For example, it has been shown [73] that the number of residues that belong to the nucleus of a model protein is about 5%; we expect the same low

percentage of residues that determine the kinetics of real proteins. The number of key residues that form a functional site is also a small fraction of the total number of residues in proteins.

In order to demonstrate the statistical significance of the outliers’ kinetic importance, we show that the number of sites with high values of ϕ found among the outliers is larger than that expected if such sites were randomly distributed across all values of S_P . For *Tenascin*, the total number of residues is $N_{tot} = 89$, the number of sites with $\phi > 0.2$ is $N_{tot}(\phi > 0.2) = 17$, the number of outliers is $N_{out} = 13$, and the expected number of sites with $\phi > 0.2$ among outliers is $N_{out}^{exp}(\phi > 0.2) = N_{tot}(\phi > 0.2)N_{out}/N_{tot} \approx 2.5$. The observed number of sites with $\phi > 0.2$ among outliers is $N_{out}(\phi > 0.2) = 8$, which is over three times more than expected. A similar estimate for $\phi > 0.5$ gives $N_{out}^{exp}(\phi > 0.5) = 0.75$ and $N_{out}(\phi > 0.5) = 2$, which is nearly three times more than expected. For *CheY*, the total number of residues is $N_{tot} = 128$, the number of sites with $\phi > 0.3$ is $N_{tot}(\phi > 0.3) = 11$, the number of outliers: $N_{out} = 22$, and the expected number of sites with $\phi > 0.3$ among outliers is $N_{out}^{exp}(\phi > 0.3) = N_{tot}(\phi > 0.3)N_{out}/N_{tot} \approx 1.9$. The observed number of sites with $\phi > 0.3$ among outliers is $N_{out}(\phi > 0.3) = 4$, which is over two times more than expected. These crude estimates demonstrate that outliers have, in fact, a higher than expected number of residues with pronounced kinetic role, hinting towards an additional evolutionary pressure exerted on kinetically important amino acids.

F. Convergent or divergent evolution?

It has been a long-standing question [9,11,74–76] whether the presently known proteins have evolved from a smaller family of prebiotic proteins (“divergent” evolution scenario) or whether they evolved from ancestors with distant homology and due to thermodynamic, kinetic, and functional pressure exerted by evolution they *converged* to structurally similar proteins (“convergent” evolution scenario). The model of evolution, proposed in this work does not rule out any of these scenarios. However, the similarity in distribution of hamming distances in the family of homologous proteins produced by our model to that taken from nature is striking (Fig. 6), serving as a hint in favor of divergent evolution.

An important argument favoring diverging evolution is that a function of a protein is strongly susceptible to protein structure [11,14]. So, if a protein were to change the structure in the course of evolution, it would affect its functionality (there are, of course, possible exceptions). Functionless genes have little chance of surviving in cells, so these proteins would most probably be eliminated. However, Murzin [11] proposed a way for functionless protein to survive by fusion with another functional protein and evolving already as a unit to a multifunctional protein. One of the most prominent examples are the DNA polymerases that are composed of similar domains with different sequence composition [77–79].

If we set aside multi-domain proteins, the fact that there is a limited amount of folds ($< 1,000$ according to Chothia [2] or $< 7,920$ according to Orengo [4]) has been extensively used to favor convergent evolution [3,6,8,10,13]. Li et al. [8] used the designability principle to show from full enumeration of lattice protein models that the number of members of a fold family depends on the stability gap Δ . This dependence means that many unrelated sequences search in the course of evolution for the stable conformations and as soon as they reach a basin of a certain fold with large enough energy gap they stay within that basin. The scenario proposed by [3,6,8] also explains why various fold families are unequally populated [4] — the number of family members depends on the energy gap. The more pronounced the energy gap is the more mutations such a fold can tolerate. Buchler and Goldstein [13] argued that the energy gap depends on the number of non-local contacts of a given fold.

There are several questions about that scenario. First, it is not clear if nature exploits all possible folds [4]: even though there are only 1,000 folds [2], it is possible that nature simply does not need more of them. Second, Chothia and Gerstein [10] argued that the restriction on the divergence of proteins from one another does not come from a stability requirement (which is of course important) but from the separation of the mutated residue from the active site. Thus, the extent of sequence divergence is inversely proportional to that of protein function(s). The experiments by Gassner et al. [80] and Axe et al. [81] support the arguments of Chothia and Gerstein [10]. In these experiments substitution of the several amino acids in the hydrophobic core of the T4 lysozyme conserved to a certain extent the function and the structure of the protein. Third, we note that there is a limited amount of types of chemical elements that are part of the ligand structures that are bound by the active site. Thus, we expect that there are groups of evolutionary unrelated proteins with similar binding sites and the structures. In fact, there are examples of proteins sharing the same site, also called a “super-site”. For example, both transforming protein p21H-RAS-1 fragment (pdb:1CTQA) and chemotactic protein 3CHY have similar binding sites, the root-mean-square deviation of one protein from another is 3.2\AA while there are only 13 identical residues (i.e. $ID < 10\%$). Interestingly, the

active site of 1CTQA is centered around Mg^{2+} , while the active site of 3CHY is built by residues only (Asp12, Asp13, Met17, and Asp57).

It is possible that evolution follows several paths at the same time and the question of whether evolution is divergent or convergent is just ill-posed. To answer this, we still need more evidence to rule out one scenario or another.

V. CONCLUSION

To conclude, we present a hierarchical model that attempts to explain sequence conservation caused by the most basic and universal evolutionary pressure in proteins to maintain stability. Using this model, we show that separation of basic time scales (that constitute a broad distribution with long tails) in evolution is a plausible scenario for the sequence heterogeneity of structurally homologous proteins. The two basic time scales are τ_o and $\tau \gg \tau_o$; *(i)* at time scales, τ_o , most mutations that occur in protein sequences do not alter the protein’s thermodynamically and/or kinetically important sites and form families of homologous proteins; *(ii)* at time scales $\tau \gg \tau_o$ mutations occur that would alter several amino acids at the important sites of the proteins in such a way that the properties of the proteins are not compromised. At time scale τ the family of analogs is formed. Mutational rates, directly computed during Z-score design, show agreement with the conservatism profiles of the fold families.

The profile solution predicts sequence entropy reasonably well for the majority, but not all, of amino acids. The amino acids that exhibit considerably higher conservatism than predicted from stability pressure alone are likely to be important for function and/or folding. Comparison of the “base-level” stability conservatism $S_P(k)$ with $S_{acr}(k)$ - actual conservatism profile of a protein fold - allows one to identify functionally and kinetically important amino acid residues and potentially gain specific insights into folding and function of a protein.

Analysis of the correlation function confirms *(i)* the presence of an intrinsic time scale, τ_o , at which designed sequences are similar and beyond which they differ strongly, *(ii)* the presence of the conserved positions in the course of Z-score design. The distributions of hamming distances between sequences reveal “clustering” of similar sequences (with low Hd) at short time scales $\tau \sim \tau_o$ and disappearance of similarity at larger time scales $\tau \gg \tau_o$. The above distributions are in accord with the distribution of hamming distances in the families of homologs, taken from the HSSP database, and with that of analogs, taken from the FSSP database, correspondingly.

The proposed study offers a plausible explanation of the clustering of structurally similar protein into families of homologs and analogs. From the perspective of the proposed view of evolution, the conservative amino acids appear as thermodynamically and kinetically important centers, mutations of which result in other (possibly strong) sequence modifications to preserve the physical properties of the parental proteins. Such modifications result in a new family of homologous proteins. In addition, the proposed model can be utilized to search for the thermodynamically and kinetically important amino acids in silica.

Evolution is an extremely complex phenomenon, driven by numerous factors, such as history, preservation of function, folding kinetics and stability of proteins in response to change in cell/body environment. It is remarkable however, that our simple model was able to qualitatively capture certain aspects of protein evolution without any adjustable parameters (except for the contact definition threshold and the empirical matrix of amino acid pairwise interactions).

In addition, our model offers an additional hint favoring a divergent evolution. However, the question of whether evolution follows a divergent or convergent path is yet to be resolved. Extensive theoretical, phenomenological and experimental effort may bring insight to this puzzle.

VI. METHODS

A. Protein model

We use the C_β representation of proteins in which each pair of amino acids is in contact if their C_β s (C_α in the case of Gly) are within the distance 7.5Å [82]. We use Miyazawa-Jernigan (MJ) [68] matrix of pair potentials to represent the interaction between each pair of 20 amino acids. The total potential energy of the protein can be written as follows:

$$E = \frac{1}{2} \sum_{i \neq j}^N U(\sigma_i, \sigma_j) \Delta_{ij}, \quad (19)$$

where N is the length of the protein, σ_i is an amino acid at the position $i = 1, \dots, N$. $U(\sigma_i, \sigma_j)$ is the corresponding element of the MJ matrix of pairwise interactions between amino acids σ_i and σ_j . Δ_{ij} is the element of the contact matrix, that is defined to be 1 if contact between amino acids i and j exists (i. e. the distance between these amino acids in the native (ground) state is smaller than 7.5 Å), and 0, if the above contact does not exist:

$$\Delta_{ij} \equiv \begin{cases} 1, & |r_i^{NS} - r_j^{NS}| \leq 7.5 \text{Å} \\ 0, & |r_i^{NS} - r_j^{NS}| > 7.5 \text{Å}, \end{cases} \quad (20)$$

where r_i^{NS} is the position of the i^{th} residue when the protein is in the native conformation.

B. The 6-letter potential

Due to the similarities in properties of the 20 types of amino acids, one can classify these amino acids into 6 distinct groups: aliphatic $\{AVLIMC\}$, aromatic $\{FWYH\}$, polar $\{STNQ\}$, positive $\{KR\}$, negative $\{DE\}$, and special (reflecting their special conformational properties) $\{GP\}$. We construct the potential of interaction, $U_6(\hat{\sigma}_i, \hat{\sigma}_j)$, between the six groups of amino acids, $\hat{\sigma}$, by computing the average interaction between these groups, i. e.

$$U_6(\hat{\sigma}_i, \hat{\sigma}_j) = \frac{1}{N_{\hat{\sigma}_i} N_{\hat{\sigma}_j}} \sum_{\sigma_k \in \hat{\sigma}_i, \sigma_l \in \hat{\sigma}_j} U_{20}(\sigma_k, \sigma_l), \quad (21)$$

where σ denotes amino acids in 20-letter representation and $U_{20}(\sigma_k, \sigma_l)$ is the 20-letter matrix of interaction MJ; $\hat{\sigma}$ denotes amino acids in 6-letter representation. $N_{\hat{\sigma}}$ is the number of actual amino acids of type $\hat{\sigma}$, e. g. for the aliphatic group $N_{\hat{\sigma}} = 6$. The 6-letter interaction potential for MJ 20-letter potential is given in Table II.

C. The measure of the information context of the sequences

In both the Z -score model and the profile solution, to study the information context of the sequences, we compute the sequence entropy, $S_X(k)$, at each position, k , of the sequence,

$$S_X(k) = - \sum_{\sigma} P_X(\sigma_k) \ln P_X(\sigma_k), \quad (22)$$

where $P_X(\sigma_k)$ is the probability that we observe an amino acid σ_k at the k th position. Subscript $X = Z$ or P denotes the Z -score model or profile solution correspondingly. The summation is taken over all possible values of σ_k .

The effect of switching to a 6-letter representation of amino acids from the 20-letter representation on the sequence entropy, $S_6(k)$, is that all values $S_6(k)$ are typically smaller than that of $S_{20}(k)$. For a M -letter alphabet with all letters equally represented, i. e. $P_X(\sigma_k) = 1/M$, the entropy is equal to $\ln M$. Thus, we expect that the difference between the typical values of $S_{20}(k)$ and $S_6(k)$ is approximately $\ln(20/6) \approx 1.2$. The case when all letters of a M -letter alphabet are equally presented corresponds to the maximal value of the entropy, i. e.

$$S_M(k) \leq \ln M. \quad (23)$$

D. The entropy of the protein fold families

Theoretical predictions from statistical-mechanical analysis can be compared with data on real proteins. In order to determine conservatism in real proteins we assume that the space of sequences that fold into the same protein structure presents a two-tier system, where homologous sequences are grouped into families and there is no recognizable sequence homology between families despite the fact that they fold into closely related structures [9,30,83].

Using the database of protein families with close sequence similarity (HSSP database [19]), we compute frequencies of amino acids at each position, k , of aligned sequences, $P_m(\sigma_k)$, for a given, m th, family of proteins. We average these frequencies *across* all N_s families sharing the same fold that are present in FSSP database [22]:

$$P_{acr}(\sigma_k) = \frac{1}{N_s} \sum_{m=1}^{N_s} P_m(\sigma_k). \quad (24)$$

Next, we determine the sequence entropy, $S_{acr}(k)$, at each position, k , of structurally aligned protein analogs:

$$S_{acr}(k) = - \sum_{\sigma} P_{acr}(\sigma_k) \ln P_{acr}(\sigma_k). \quad (25)$$

VII. ACKNOWLEDGMENTS

We thank R. S. Dokholyan for careful reading of the manuscript and S. V. Buldyrev, A. V. Finkelstein, A. Yu. Grosberg, and L. A. Mirny for helpful discussions. The profile solution was developed in [50] with L. A. Mirny. NVD is supported by NIH postdoctoral fellowship GM20251-01. EIS is supported by NIH grant RO1-52126.

APPENDIX A: DETERMINATION OF CONTACT FREQUENCIES FROM HOMOPOLYMER CONFORMATIONS

The estimation of frequencies is one of the key ingredients in protein design. An alternative approach to that proposed above is to assume that the set of conformational decoys is the set of all possible random coil states of a homopolymer collapsed at the temperatures below theta-point temperature, $T < T_{\theta}$ — these are the states that decoy random heteropolymers explore at the folding transition temperature. Thus, we can determine the frequencies of contacts in an ensemble of random heteropolymers by taking the time average of a contact matrix element Δ_{ij} in the possible conformations of a homopolymer at $T < T_{\theta}$.

To compute the frequencies of contacts for a homopolymer of length N , we use discrete molecular dynamics simulations [73,84,85]. We model a homopolymer by N beads on a string with the interaction distances scaled to 7.5Å. (see [85] for a detailed description of the model and the algorithm). We run the simulation at the temperature T_{θ} (ϵ parameter [85] is set to -1) for 10^7 time units¹. After 10^7 time units of simulations we compute the frequency f_{ij} of each of the $N(N-1)/2$ contacts in our homopolymer.

There are two principal drawbacks of the second method: (1) the probability of occurrence of stable elements of the structure in homopolymers resembling secondary structure in proteins is so low that the distribution of contact lengths, $P(\ell)$, in homopolymer (not shown) drastically differs from that shown for real proteins in Fig. 3. (2) The model of a homopolymer used in the simulations strongly differs (e.g. in flexibility) from real proteins. In fact, the problem of building an appropriate model for chain flexibility is so important that small variations in it result in drastically different kinetics from a realistic one (e.g. appearance of the intermediate states) [86,87]. We find that both of these drawbacks make the “homopolymer” approach of estimating the frequencies very inefficient for existing protein models, so we omit it in our studies.

There are two strong advantages of this approach, which make it worthwhile to explore it in the future, upon the availability of the realistic protein models: (i) the possibility to generate a large amount of decoy conformations and, thus, achieve statistically highly significant contact frequency spectra; (ii) the independence of the produced decoys from various database biases.

-
- [1] Levitt, M. & Chothia, C. (1976). Structural patterns in globular proteins. *Nature* **261**, 552–558.
 - [2] Chothia, C. (1992). One thousand families for the molecular biologist. *Nature* **357**, 543–544.
 - [3] Finkelstein, A. V., Gutin, A., & Badretdinov, A. (1993). Why are some protein structures so common?. *FEBS Letters* **325**, 23–28.
 - [4] Orengo, C. A., Jones, D. T., & Thornton, J. M. (1994). Protein superfamilies and domain superfolds. *Nature* **372**, 631–634.
 - [5] Davidson, A. R. & Sauer, R. T. (1994). Folded proteins occur frequently in libraries of random amino acid sequences. *Proc. Natl. Acad. Sci. U. S. A.* **91**, 2146–2150.

¹In the discrete molecular dynamics algorithm, the time unit is the average time between subsequent collisions

- [6] Finkelstein, A. V., Gutin, A., & Badretdinov, A. (1995). Why are the same protein folds used to perform different functions?. *Proteins* **23**, 142–149.
- [7] Murzin, A. G., Brenner, S. E., Hubbard, T., & Chothia, C. (1995). Scop: A structural classification of proteins database for the investigation of sequences and structures. *J. Mol. Biol.* **247**, 536–540.
- [8] Li, H., Helling, R., Tang, C., & Wingreen, N. S. (1996). Emergence of preferred structures in a simple model of protein folding. *Science* **273**, 666–669.
- [9] Rost, B. (1997). Protein structures sustain evolutionary drift. *Folding & Design* **2**, S19–S24.
- [10] Chothia, C. & Gerstein, M. (1997). Protein evolution - how far can sequences diverge?. *Nature* **385**, 579.
- [11] Murzin, A. G. (1998). How far divergent evolution goes in proteins. *Curr. Opinion Struc. Biol.* **8**, 380–387.
- [12] Holm, L. (1998). Unification of protein families. *Curr. Opinion Struc. Biol.* **8**, 372–379.
- [13] Buchler, N. E. G. & Goldstein, R. A. (2000). Surveying determinants of protein structure designability across different energy models and amino-acid alphabets: A consensus. *J. Chem. Phys.* **112**, 2533–2547.
- [14] Alberts, B., Bray, D., Lewis, J., Raff, M., Roberts, K., & Watson, J. D. (1994). *Molecular biology of the cell*. Garland Publishing, New York.
- [15] Sander, C. & Schneider, R. (1991). Database of homology-derived protein structures and the structural meaning of sequence alignment. *Proteins* **9**, 56–68.
- [16] Flaherty, K. M., McKay, D. B., Kabsch, W., & Holmes, K. C. (1991). Similarity of the three-dimensional structures of actin and the atpase fragment of a 70k heat-shock cognate protein. *Proc. Natl. Acad. Sci. U. S. A.* **88**, 5041–5045.
- [17] Holmes, K. C., Sander, C., & Valencia, A. (1993). A new atp-binding fold in actin , hexokinase and hsc70. *Trends Cell Biol.* **3**, 53–59.
- [18] Orengo, C. A., Michie, A. D., Jones, S., Jones, D. T., Swindells, M. B., & Thornton, J. M. (1997). Cath – a hierarchic classification of protein domain structures. *Structure* **5**, 1093–1108.
- [19] Dodge, C., Schneider, R., & Sander, C. (1998). The hssp database of protein structure-sequence alignments and family profiles. *Nucl. Acid Res.* **26**, 313–315.
- [20] Sánchez, R., Pieper, U., Melo, F., Eswar, N., Marti-Renom, M. A., Madhusudhan, M. S., Mirković, N., & Sali, A. (2000). Protein structure modeling for structural genomics. *Nature Struct. Biol.* **7**, 986–990.
- [21] Perl, F. M. G., Lee, D., Bray, J. E., Sillitoe, I., Todd, A. E., Harrison, A. P., Thornton, J. M., & Orengo, C. A. (2000). Assigning genomic sequences to cath. *Nucl. Acid Res.* **28**, 277–282.
- [22] Holm, L. & Sander, C. (1993). Protein structure comparison by alignment of distance matrices. *J. Mol. Biol.* **233**, 123–138.
- [23] Holm, L. & Sander, C. (1997). An evolutionary treasure: unification of a broad set of amidohydrolases related to urease. *Proteins* **28**, 72–82.
- [24] Shakhnovich, E. I. & Gutin, A. M. (1993). Engineering of stable and fast folding sequences of model proteins. *Proc. Natl. Acad. Sci. U. S. A.* **90**, 7195–7199.
- [25] Abkevich, V. I., Gutin, A. M., & Shakhnovich, E. I. (1996). Improved design of stable and fast-folding model proteins. *Folding & Design* **1**, 221–230.
- [26] Shakhnovich, E. I. (1997). Theoretical studies of protein-folding thermodynamics and kinetics. *Curr. Opinion Struc. Biol.* **7**, 29–40.
- [27] Bryngelson, J. D. & Wolynes, P. G. (1987). Spin glasses and the statistical mechanics of protein folding. *Proc. Natl. Acad. Sci. U. S. A.* **84**, 7524–7528.
- [28] Abkevich, V. I., Gutin, A. M., & Shakhnovich, E. I. (1998). Theory of kinetic partitioning in protein folding with possible applications to prions. *Proteins: Struc. Func. Genet.* **31**, 335–344.
- [29] Shakhnovich, E. I. (1998). Protein design: a perspective from simple tractable models. *Folding & Design* **3**, R45–R58.
- [30] Mirny, L. A. & Shakhnovich, E. I. (1999). Universally conserved positions in protein folds: reading evolutionary signals about stability, folding kinetics and function. *J. Mol. Biol.* **291**, 177–196.
- [31] Altschuh, D., Vernet, T., Berti, P., Moras, D., & Nagai, K. (1988). Coordinated amino acid changes in homologous protein families. *Protein Eng.* **2**, 193–199.
- [32] Thomas, D., Casari, G., & Sander, C. (1996). The prediction of protein contacts from multiple sequence alignments. *Protein Eng.* **9**, 941–948.
- [33] Gutin, A. M., Sali, A., Abkevich, V. I., Karplus, M., & Shakhnovich, E. I. (1998). Temperature dependence of the folding rate in a simple protein model: Search for a "glass" transition. *J. Chem. Phys.* **108**, 6466–6483.
- [34] Buchler, N. E. G. & Goldstein, R. A. (1999). Universal correlation between energy gap and foldability for the random energy model and lattice proteins. *J. Chem. Phys.* **111**, 6599–6609.
- [35] Mirny, L. A., Finkelstein, A. V., & Shakhnovich, E. I. (2000). Statistical significance of protein structure prediction by threading. *Proc. Natl. Acad. Sci. U. S. A.* **97**, 9978–9983.
- [36] Bernstein, F. C., Koetzle, T. F., Williams, G. J. B., Jr., E. F. M., Brice, M. D., Rodgers, J. R., Kennard, O., Shimanouchi, T., & Tasumi, M. (1977). The protein data bank: a computer-based archival file for macromolecular structures. *J. Mol. Biol.* **112**, 535–542.
- [37] Abola, E. E., Bernstein, F. C., Bryant, S. H., Koetzle, T. F., & Weng, J. (1987). in *Crystallographic Databases-Information Content, Software Systems, Scientific Applications* (Allen, F. H., Bergerhoff, G., & Sievers, R., eds.) pp. 107–132. Data Commission of the International Union of Crystallography, Cambridge.
- [38] Ramanathan, S. & Shakhnovich, E. I. (1994). Statistical mechanics of proteins with evolutionary "selected" sequences.

Phys. Rev. E **50**, 1303–1312.

- [39] Sali, A., Shakhnovich, E. I., & Karplus, M. (1994). Kinetics of protein folding. a lattice model study for the requirements for folding to the native state. *J. Mol. Biol.* **235**, 1614–1636.
- [40] Pande, V. S., Grosberg, A. Y., & Tanaka, T. (1995). Freezing transition of random heteropolymers consisting of arbitrary sets of monomers. *Phys. Rev. E* **51**, 3381–3393.
- [41] Saven, J. & Wolynes, P. (1997). Statistical mechanics of the combinatorial synthesis and analysis of folding molecules. *J. Phys. Chem. B* **101**, 8375–8389.
- [42] Bowie, J. U., Luthy, R., & Eisenberg, D. (1991). A method to identify protein sequences that fold into a known 3-dimensional structure. *Science* **253**, 164–170.
- [43] Press, W. H., Flannery, B. P., Teukolsky, S. A., & Vetterling, W. T. (1989). *Numerical recipes*. Cambridge University Press, Cambridge.
- [44] Shakhnovich, E. I. & Gutin, A. M. (1989). Formation of unique structure in polypeptide chains: Theoretical investigation with the aid of a replica approach. *Biophys. Chem.* **34**, 187–199.
- [45] Shakhnovich, E. I. & Gutin, A. M. (1990). Implications of thermodynamics of protein folding for evolution of primary sequences. *Nature* **346**, 773–775.
- [46] Pande, V. S., Grosberg, A. Y., & Tanaka, T. (1997). Statistical mechanics of simple models of protein folding and design. *Biophys. J.* **73**, 3192–3210.
- [47] Ptitsyn, O. B. (1998). Protein folding and protein evolution: Common folding nucleus in different subfamilies of c-type cytochromes?. *J. Mol. Biol.* **278**, 655–666.
- [48] Mirny, L. A., Abkevich, V. I., & Shakhnovich, E. I. (1998). How evolution makes proteins fold quickly. *Proc. Natl. Acad. Sci. U. S. A.* **95**, 4976–4981.
- [49] Ptitsyn, O. B. & Ting, K.-L. H. (1999). Non-functional conserved residues in globins and their possible role as a folding nucleus. *J. Mol. Biol.* **291**, 671–682.
- [50] Dokholyan, N. V., Mirny, L. A., & Shakhnovich, E. I. (2000b). Understanding conserved amino acids in proteins. **cond-mat/0007084**.
- [51] Krebs, H., Schmid, F. X., & Jaenicke, R. (1983). Folding of homologous proteins. *J. Mol. Biol.* **169**, 619–635.
- [52] Lesk, A. M. & Chothia, C. (1980). How different amino acid sequences determine similar protein structures: the structure and evolutionary dynamics of the globins. *J. Mol. Biol.* **136**, 225–270.
- [53] Hollecker, M. & Creighton, T. E. (1983). Evolutionary conservation and variation of protein folding pathways. *J. Mol. Biol.* **168**, 409–437.
- [54] Plaxco, K. W., Spitzfaden, C., Campbell, I. D., & Dobson, C. M. (1997). A comparison of the folding kinetics and thermodynamics of two homologous fibronectin type iii modules. *J. Mol. Biol.* **270**, 763–770.
- [55] Nishimura, C., Prytulla, S., Dyson, H. J., & Wright, P. E. (2000). Conservation of folding pathways in evolutionarily distant globin sequences. *Nature Struct. Biol.* **7**, 679–686.
- [56] Lorch, M., Mason, J., Clarke, A., & Parker, M. (1999). Effects of core mutations on the folding of a beta-sheet protein: implications for backbone organization in the i-state. *Biochemistry* **38**, 1377–1385.
- [57] Schindler, T., Perl, D., Graumann, P., Sieber, V., Marahiel, M., & Schmid, F. (1998). Surface-exposed phenylalanines in the rnp1/rnp2 motif stabilize the cold-shock protein cspb from *bacillus subtilis*. *Proteins: Struct. Func. Genet.* **30**, 401–406.
- [58] López-Hernández, E. & Serrano, L. (1996). Structure of the transition state for folding of the 129 aa protein chy resembles that of a smaller protein, ci-2. *Folding & Design* **1**, 43–55.
- [59] Russell, R., Sasieni, P., & Sternberg, M. (1998). Supersites within superfolds. Binding site similarity in the absence of homology. *J. Mol. Biol.* **282**, 903–918.
- [60] Welch, M., Oosawa, K., Aizawa, S., & Eisenbach, M. (1994). Effects of phosphorylation, mg^{2+} , and conformation of the chemotaxis protein chey on its binding to the flagellarswitch protein film. *Biochemistry* **33**, 10470–10476.
- [61] Bellolell, L., Cronet, P., Majolero, M., Serrano, L., & Coll, M. (1996). The three-dimensional structure of two mutants of the signal transduction protein chey suggests its molecular activation mechanism. *J. Mol. Biol.* **257**, 116–128.
- [62] Wilcock, D., Pissabarro, M. T., López-Hernández, E., Serrano, L., & Coll, M. (1998). Structure analysis of two chey mutants: importance of the hydrogen bond contribution to protein stability. **54**, 378–385.
- [63] Villegas, V., Martínez, J. C., Avilés, F. X., & Serrano, L. (1998). Structure of the transition state in the folding process of human procarboxypeptidase a2 activation domain. *J. Mol. Biol.* **283**, 1027–1036.
- [64] van Nuland, N. A. J., Chiti, H., Taddei, N., Raugei, G., Ramponi, G., & Dobson, C. (1998a). Slow folding of muscle acylphosphatase in the absence of intermediates. *J. Mol. Biol.* **283**, 883–891.
- [65] van Nuland, N. A. J., Meijberg, W., Warner, J., Forge, V., Scheek, R., Robbilar, G., & Dobson, C. (1998b). Slow cooperative folding of a small globular protein hpr. *Biochemistry* **37**, 622–637.
- [66] Li, H., Tang, C., & Wingreen, N. S. (1997). Nature of driving force for protein folding: A result from analyzing the statistical potential. *Phys. Rev. Lett.* **79**, 765–768.
- [67] Miyazawa, S. & Jernigan, R. L. (1985). Estimation of effective interresidue contact energies from protein crystal structures: quasi-chemical approximation. *Macromolecules* **18**, 534–552.
- [68] Miyazawa, S. & Jernigan, R. L. (1996). Residue-residue potentials with a favorable contact pair term and an unfavorable high packing density term, for simulation and threading. *J. Mol. Biol.* **256**, 623–644.
- [69] Kussell, E., Shimada, J., & Shakhnovich, E. I. (2001). Excluded volume in protein sidechain packing. *J. Mol. Biol.* ,

submitted.

- [70] Itzhaki, L. S., Otzen, D. E., & Fersht, A. R. (1995). The structure of the transition-state for folding of chymotrypsin inhibitor-2 analyzed by protein engineering methods — evidence for a nucleation-condensation mechanism for protein-folding. *J. Mol. Biol.* **254**, 260–288.
- [71] Hamill, S. J., Steward, A., & Clarke, J. (2000). The folding of an immunoglobulin-like greek key protein is defined by a common-core nucleus and regions constrained by topology. *J. Mol. Biol.* **297**, 165–178.
- [72] Chiti, F., Taddei, N., White, P. M., Bucciantini, M., Magherini, F., Stefani, M., & Dobson, C. M. (1999). Mutational analysis of acylphosphatase suggests the importance of topology and contact order in protein folding. *Nature Struct. Biol.* **6**, 1005–1009.
- [73] Dokholyan, N. V., Buldyrev, S. V., Stanley, H. E., & Shakhnovich, E. I. (2000a). Identifying the protein folding nucleus using molecular dynamics. *J. Mol. Biol.* **296**, 1183–1188.
- [74] Zhang, G., Liu, Y., Ruoho, A. E., & Hurley, J. H. (1987). Structure of the adenylyl cyclase catalytic core. *Nature* **386**, 247–253.
- [75] Artymiuk, P. J., Poirrette, A. R., Rice, D. W., & Willett, P. (1997). A polymerase i palm in adenylyl cyclase?. *Nature* **388**, 33–34.
- [76] Bryant, S. H., Madej, T., Liu, Y., Ruoho, A. E., Zhang, G., & Hurley, J. H. (1997). A polymerase i palm in adenylyl cyclase? – reply. *Nature* **388**, 34.
- [77] Wang, J., Sattar, A. K. M. A., Wang, C. C., Karam, J. D., Konigsberg, W. H., & Steitz, T. A. (1997). Crystal structure of a pol α family replication dna polymerase from bacteriophage rb69. *Cell* **89**, 1087–1099.
- [78] Doublé, S., Tabor, S., Long, A. M., Richardson, C. C., & Ellenberg, T. (1997). Crystal structure of a bacteriophage t7 dna replication complex at 2.2 Å resolution. *Nature* **391**, 251–258.
- [79] Kiefer, J. R., Mao, C., Braman, J. C., & Beese, L. S. (1997). Visualizing dna replication in a catalytically active *bacillus* dna polymerase crystals. *Nature* **391**, 304–307.
- [80] Gassner, N. C., Baase, W. A., & Matthews, B. W. (1996). A test of the "jigsaw puzzle" model for protein folding by multiple methionine substitutions within the core of t4 lysozym. *Proc. Natl. Acad. Sci. U. S. A.* **93**, 12155–12158.
- [81] Axe, D. D., Foster, N. W., & Fersht, A. R. (1996). Active barnase variants with completely random hydrophobic core. *Proc. Natl. Acad. Sci. U. S. A.* **93**, 5590–5594.
- [82] Jernigan, R. L. & Bahar, I. (1996). Structure-derived potentials and protein simulations. *Curr. Opinion Struc. Biol.* **6**, 195–209.
- [83] Tiana, G., Broglia, R., & Shakhnovich, E. I. (2000). Hiking in the energy landscape in sequence space: A bumpy road to good folders. *Proteins: Struc. Func. Genet.* **39**, 244–251.
- [84] Zhou, Y. & Karplus, M. (1997). Folding thermodynamics of a three-helix-bundle protein. *Proc. Natl. Acad. Sci. U. S. A.* **94**, 14429–14432.
- [85] Dokholyan, N. V., Buldyrev, S. V., Stanley, H. E., & Shakhnovich, E. I. (1998). Molecular dynamics studies of folding of a protein-like model. *Folding & Design* **3**, 577–587.
- [86] Borreguero, J. M., Dokholyan, N. V., Buldyrev, S., Stanley, H. E., & Shakhnovich, E. I. (2001). Transition state of c-crk sh3 domain: Molecular dynamics simulations of simple models. *in preparation*.
- [87] Ding, F., Dokholyan, N. V., Buldyrev, S. V., Stanley, H. E., & Shakhnovich, E. I. (2001). Direct observation of folding transition state ensemble of c-src sh3 domain in molecular dynamics simulations. *in preparation*.
- [88] Berezovsky, I. N., Grosberg, A. Y., & Trifonov, E. N. (2000). Closed loops of nearly standard size: common basic element of protein structure. *FEBS Letters* **466**, 283–286.

Fold	N_s	Representative protein		Correlation coefficient, r			
		PDB code [36,37]	N	$R(k)$ vs. $S_{acr}(k)$	$S_P(k)$ vs. $S_{acr}(k)$	T_{sel}	$S_P(k)$ vs. $S_{acr}(k)$ ($T_{sel} = 0.25$)
Ig	51	1TEN	89	0.57	0.63	0.34	0.57
OB	18	1MJC	69	0.67	0.69	0.19	0.69
R	166	3CHY	128	0.74	0.71	0.25	0.71
α/β -P	29	2ACY	98	0.45	0.54	0.26	0.53
TIM	49	2EBN	285	0.54	0.50	0.23	0.50

TABLE I. The values of the correlation coefficient r for the linear regression of $S_P(k)$ and $R(k)$ versus S_{acr} for Ig, OB, R, α/β -P, and TIM folds and the corresponding optimal values of the temperature $T = T_{sel}$ for the $S_P(k)$ versus S_{acr} linear regression. The last column corresponds to the correlation coefficient for the studied folds at a fixed selective temperature $T = 0.25$. To obtain the rates of mutations, $R(k)$, we perform Z -score design of the sequences for $t_d = 10^8$ Monte Carlo steps at $T_{des} = 0.25$.

	l	r	p	+	-	s
l	-0.31	-0.39	-0.22	0.01	-0.41	-0.12
r	-0.39	-0.27	-0.32	-0.02	-0.28	-0.12
p	-0.22	-0.32	-0.41	-0.25	0.07	-0.29
+	0.01	-0.02	-0.25	-0.10	-0.18	-0.18
-	-0.41	-0.28	0.07	-0.18	0.01	-0.05
s	-0.12	-0.12	-0.29	-0.18	-0.05	0.04

TABLE II. A 6-letter potential derived (see Section VIB) for MJ 20-letter potential. The symbols “l”, “r”, “p”, “+”, “-” and “s” denote 6 distinct corresponding groups of amino acids: aliphatic {AVLIMC}, aromatic {FWYH}, polar {STNQ}, positively charged {KR}, negatively charged {DE}, and special (reflecting their special conformational properties) {GP}.

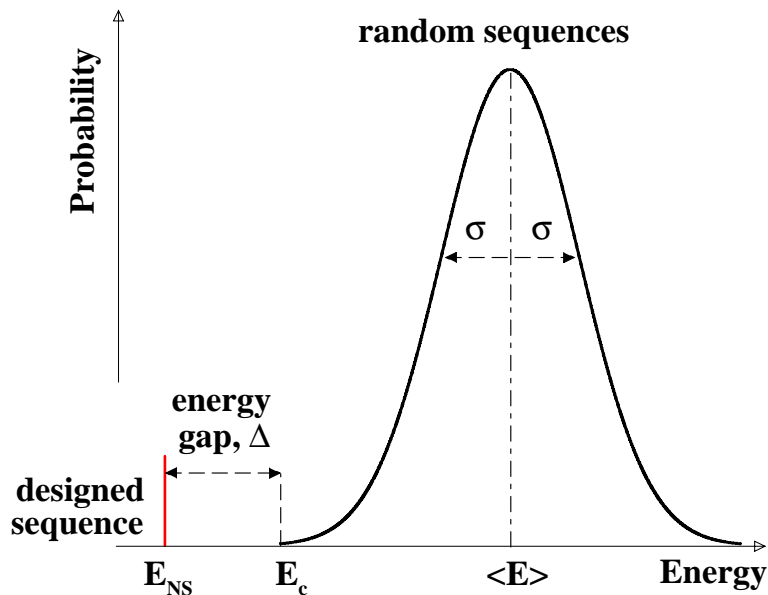


FIG. 2. A schematic representation of the probability distribution of energies of the random sequences versus the designed sequence.

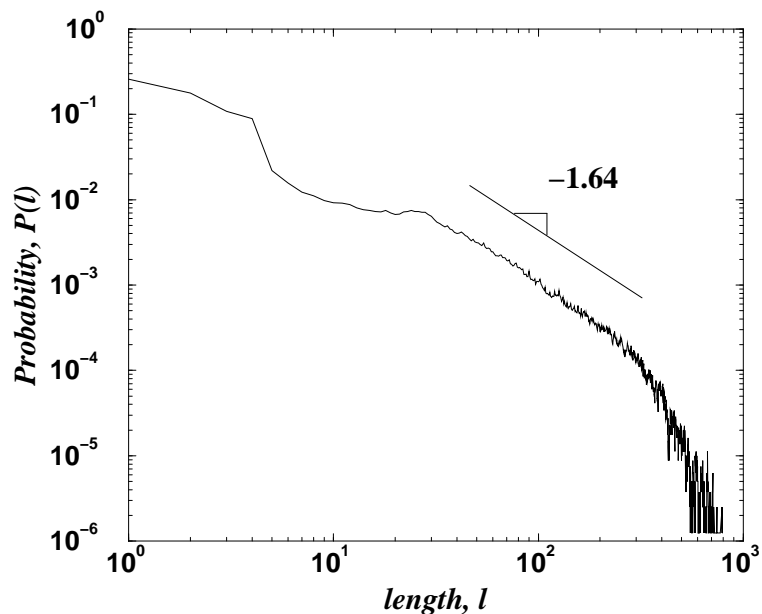


FIG. 3. Double-logarithmic plot of the distribution, $P(\ell)$, of contacts of length $\ell = |i - j|$ in the ensemble of approximately 10^3 representative globular proteins in (PDB) [36,37]. The contact between residues positioned i th and j th along the protein chain is defined by the Eq. (20) using C_β -representation of proteins. The parallel line in the range of length $20 < \ell < 200$ indicates the power-law behavior of $P(\ell)$ in this region, $P(\ell) \sim \ell^{-1.64}$. The region $5 < \ell < 20$ is specific to proteins and has been discussed in detail in [88].

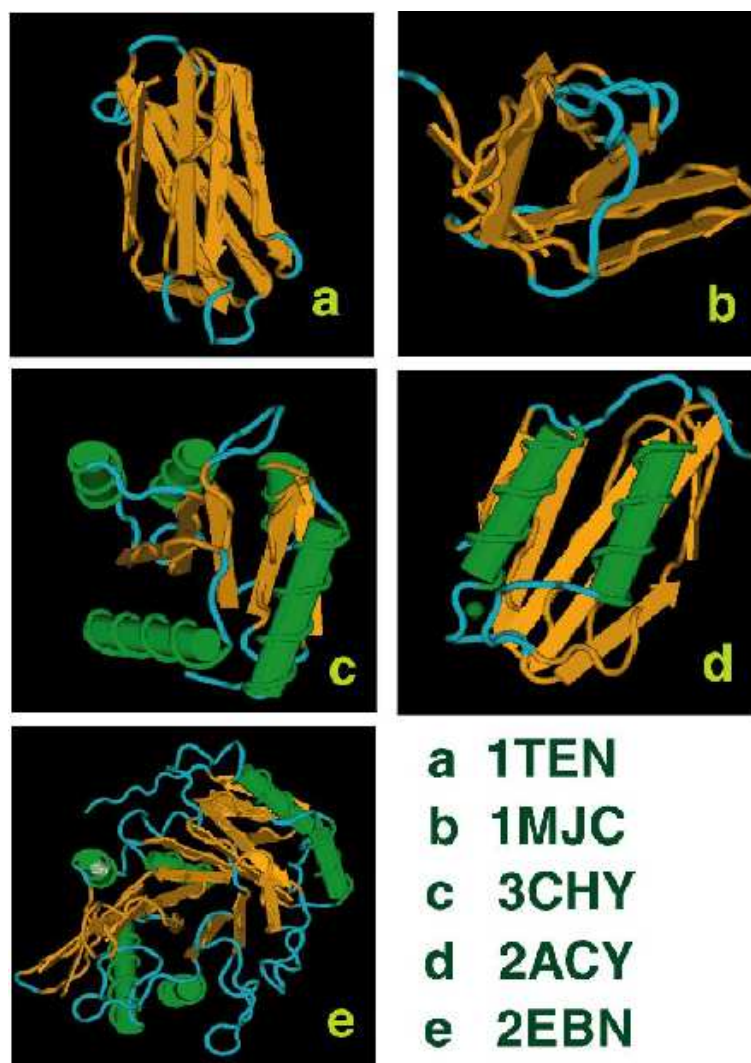


FIG. 4. Three dimensional structures of the representative proteins of the five folds under study (Ig, OB, R, α/β -P and TIM folds): (a) 1TEN protein, (b) 1MJC, (c) 3CHY, (d) 2ACY, and (e) 2EBN.

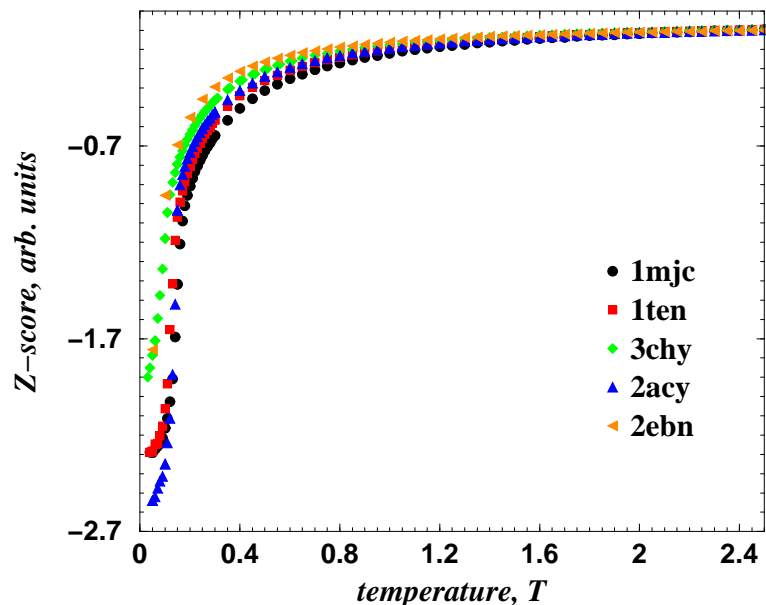


FIG. 5. The temperature dependence of the Z -score obtained after 10^5 Monte Carlo steps and averaged over 100 design “trajectories” for five representative proteins (1MJC, 1TEN, 3CHY, 2ACY, and 2EBN) of the five folds studied. Due to normalization of the contacts’ frequencies extracted from PDB database, the scales of values of Z are different from the actual Z -score with correctly normalized Z - score.

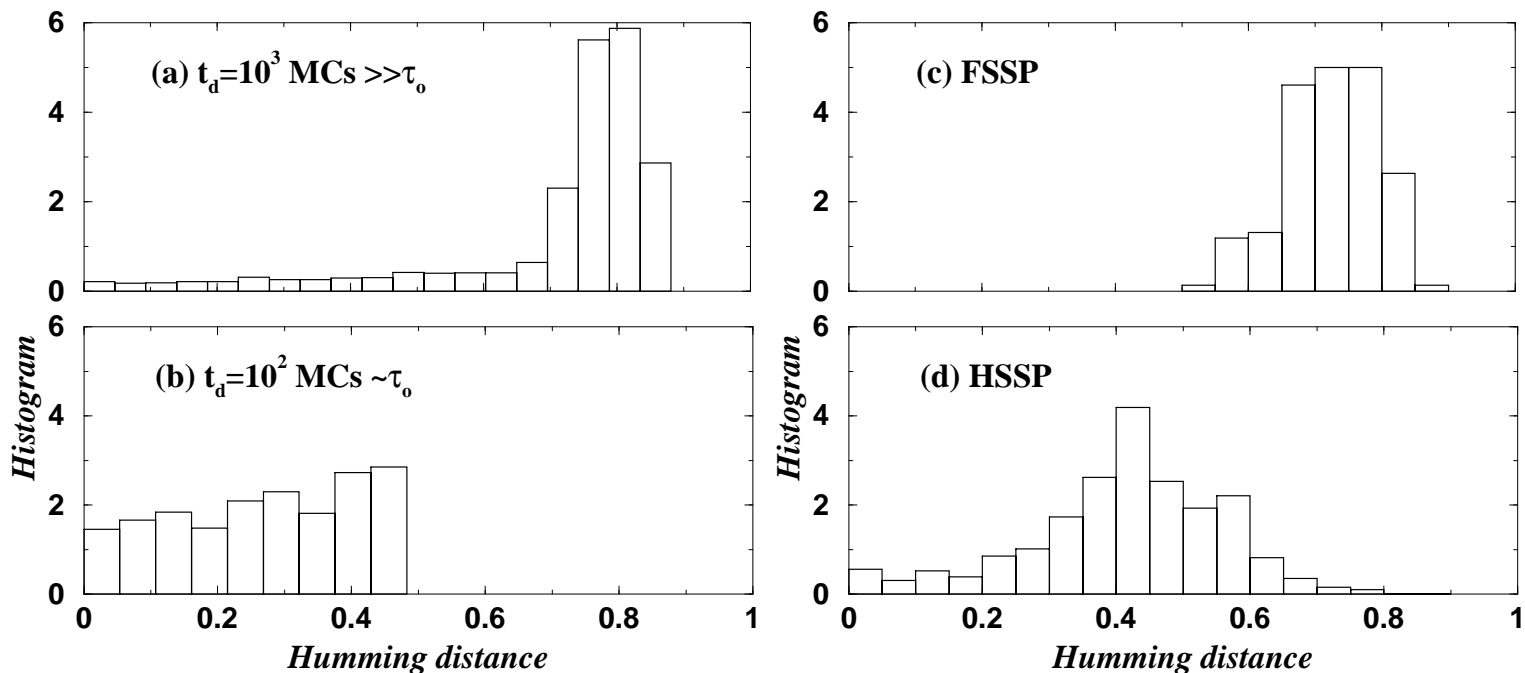


FIG. 6. The histograms of hamming distances for 1MJC family between all designed sequences for two design times (a) $t_d = 10^3 \gg \tau_o$ and (b) $t_d = 10^2 \sim \tau_o$ Monte Carlo steps. The histograms of hamming distances for 1MJC family of actual protein sequences: (c) analogs, taken from the FSSP database, and (d) homologs, taken from the HSSP database. In the computation of the histograms in case (b) we omit all sequences with sequence similarity less than $ID = 55\%$ to mimic sequence collection in the HSSP database. The threshold sequence similarity, ID , is chosen so that the hamming distance histogram derived from the actual sequences in HSSP database (d). All histograms are normalized to unit area.

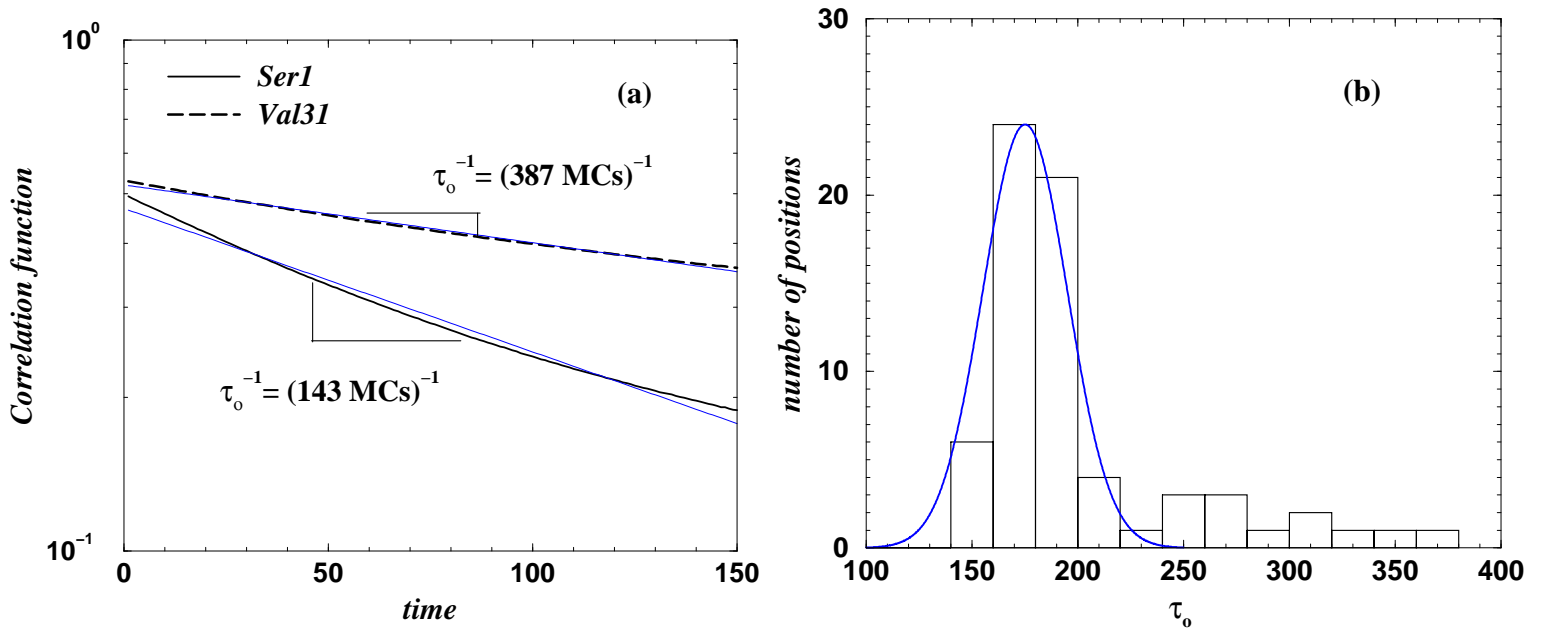


FIG. 7. (a) Plot of the correlation functions versus time for two position in 1MJC, Ser1 and Val31, obtained in the course of Z-score design of 10^3 sequences for 10^3 Monte Carlo steps. In semilogarithmic scale $C_{k=1}(\tau)$ and $C_{k=31}(\tau)$ are straight lines with slopes $\tau_o = 143$ and $\tau_o = 387$ Monte Carlo steps correspondingly. (b) The histogram of the relaxation times τ_o for all positions in 1MJC obtained in the course of Z-score design of 10^3 sequences for 10^3 Monte Carlo steps. The histogram is well fit by a Gaussian function in the region $100 < \tau_o < 250$ (solid line). The long tail that strongly deviates from the Gaussian distribution (over seven standard deviations) indicates the presence of the conserved positions in the course of design.

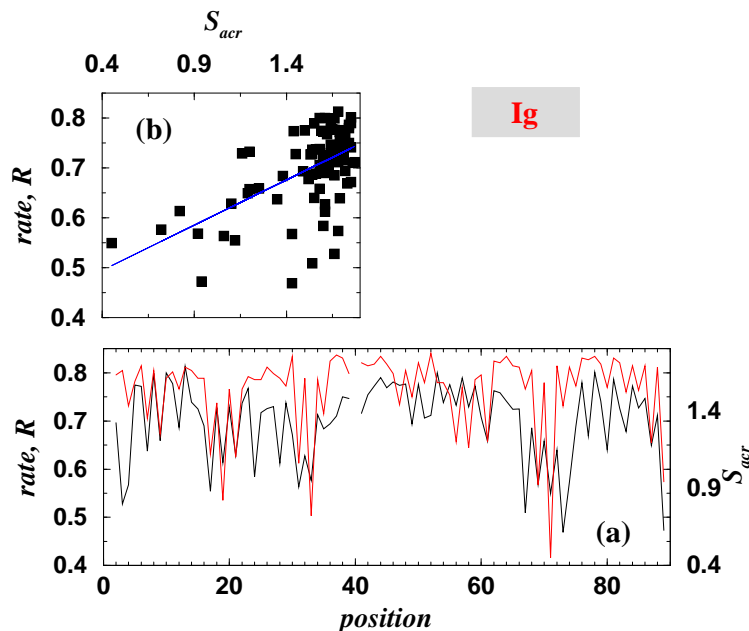


FIG. 8. (a) The values $R(k)$ (black line) and $S_{acr}(k)$ (red line) for all positions, k , for the Ig-fold. The lower the values of $R(k)$ the more conservative amino acids are at these positions. (b) The scatter plot of $R(k)$ versus observed $S_{acr}(k)$. The linear regression correlation coefficients are shown in Table I. The blue line is the linear regression approximation. In both parts (a) and (b) rates are multiplied by the length of the representative protein.

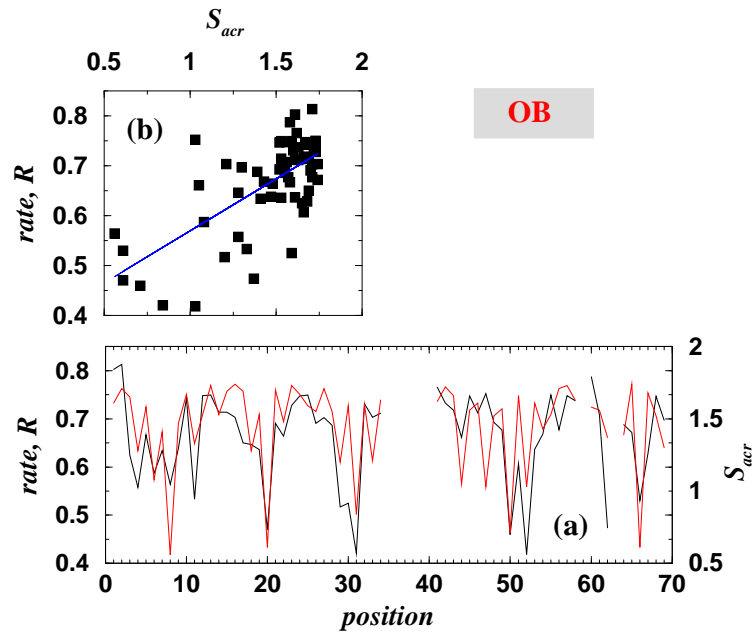


FIG. 9. (a) — (c) The same as Fig.8 but for the OB-fold.

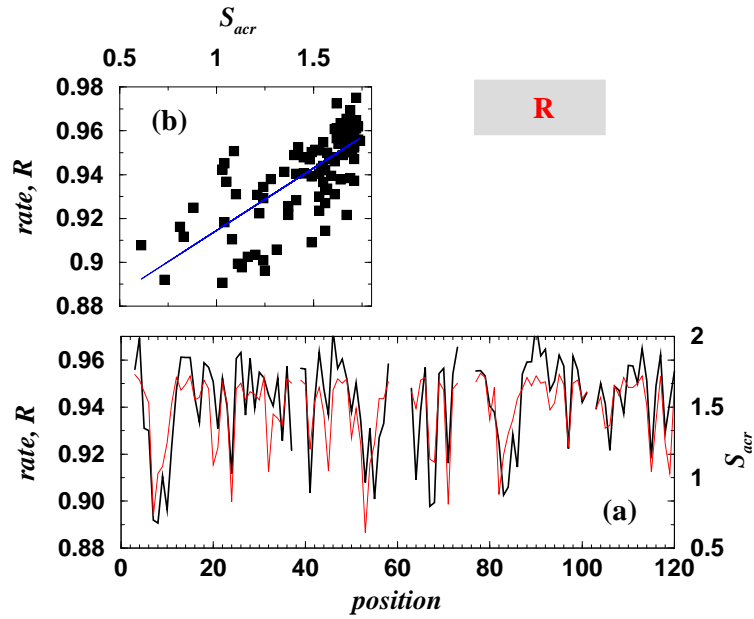


FIG. 10. (a) — (c) The same as Fig.8 but for R-fold.

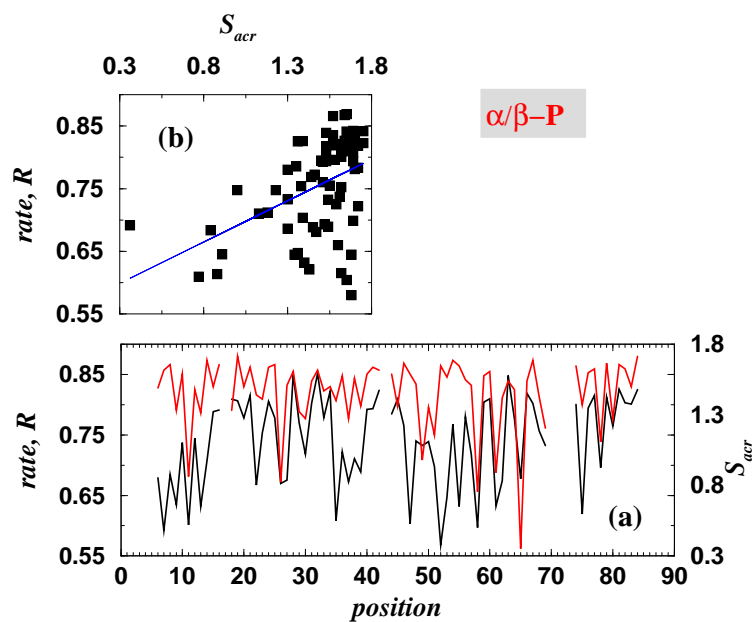


FIG. 11. (a) — (c) The same as Fig.8 but for the α/β -P-fold.

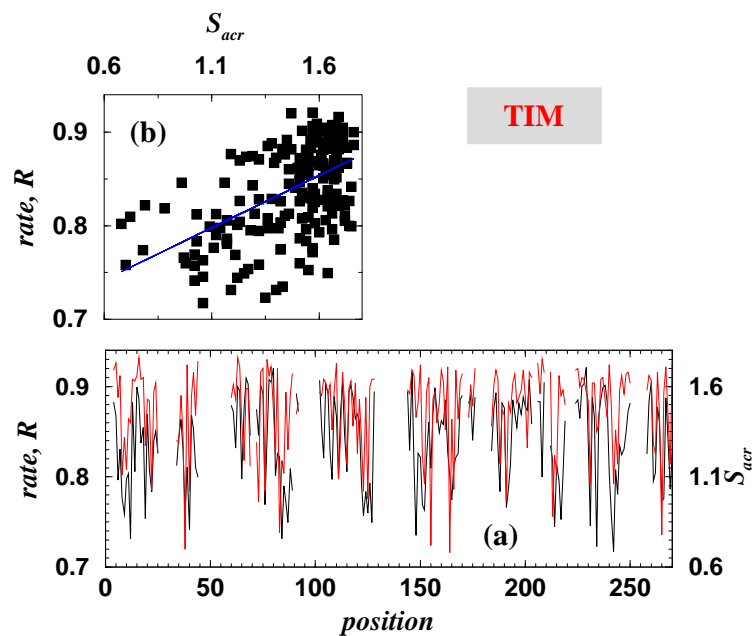


FIG. 12. (a) — (c) The same as Fig.8 but for TIM-fold.

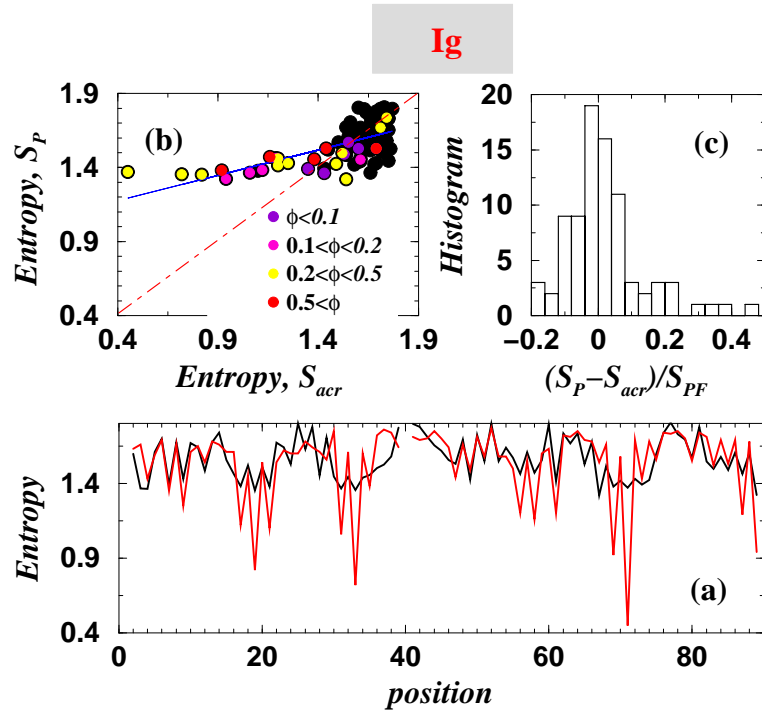


FIG. 13. (a) The values $S_P(k)$ (black line) and $S_{acr}(k)$ (red line) for all positions, k , for the Ig-fold. The lower the values of $S_P(k)$ the more conservative amino acids are at these positions. (b) The scatter plot of predicted $S_P(k)$ versus observed $S_{acr}(k)$. The linear regression correlation coefficients are shown in Table I. The blue line is the linear regression that has a slope different than 1 (red line), corresponding to the $S_P(k) = S_{acr}(k)$ relation. (c) The histogram of the relative differences between $S_P(k)$ and $S_{acr}(k)$. In (b) we assign colors to data points corresponding to amino acids with the specific range of ϕ -values [71]: red, if $0.5 < \phi < 1$, yellow, if $0.2 < \phi < 0.5$, magenta, if $0.1 < \phi < 0.2$, violet if $\phi < 0.1$, and black if ϕ -values are not determined.

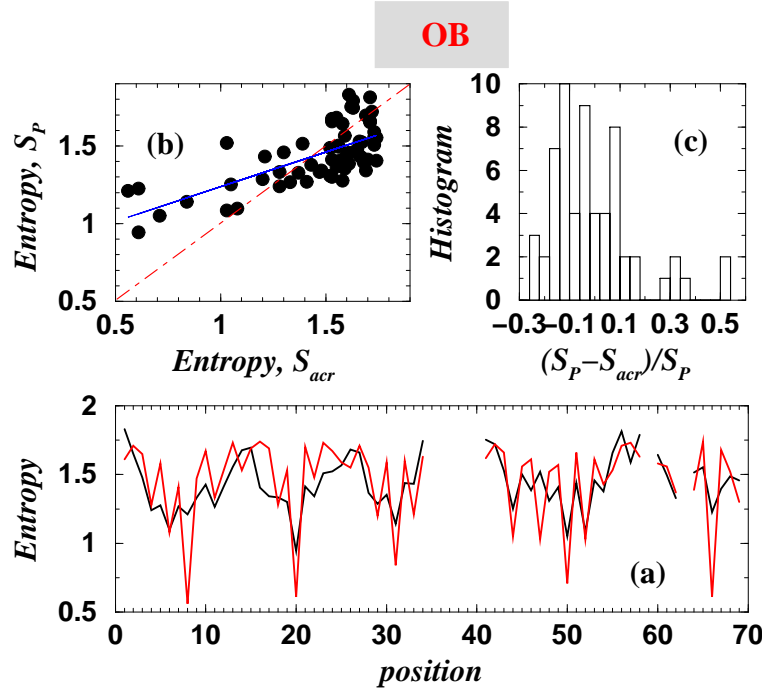


FIG. 14. (a) — (c) The same as Fig.13 but for the OB-fold.

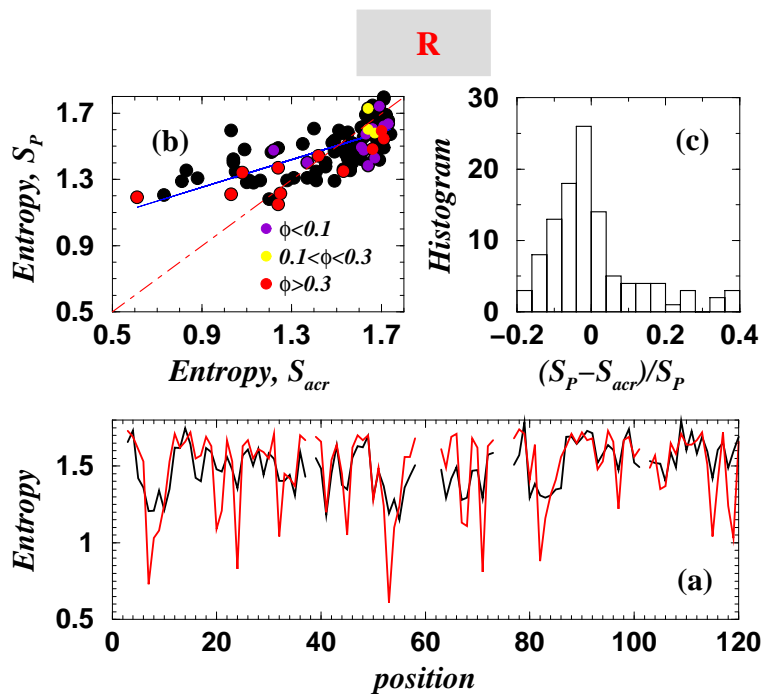


FIG. 15. (a) — (c) The same as Fig.2 but for R-fold. In (b) we assign colors to data points corresponding to amino acids with the specific range of ϕ -values [58]: red, if $0.3 < \phi < 1$, yellow, if $0.1 < \phi < 0.3$, violet if $\phi < 0.1$, and black if ϕ -values are not determined.

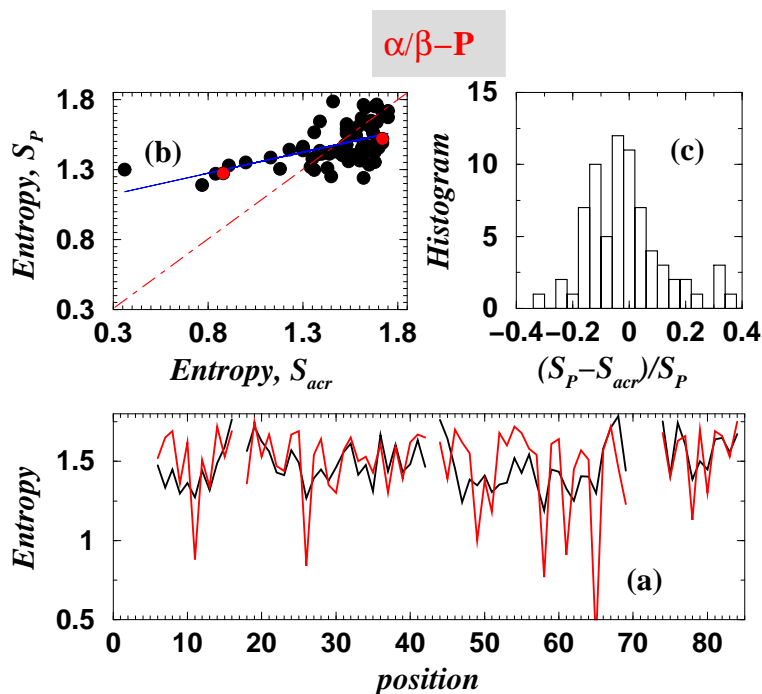


FIG. 16. (a) — (c) The same as Fig.13 but for the $\alpha/\beta - P$ -fold. In (b) we color red (2 out 3) nucleic amino acids, Tyr11 and Pro54, [72].

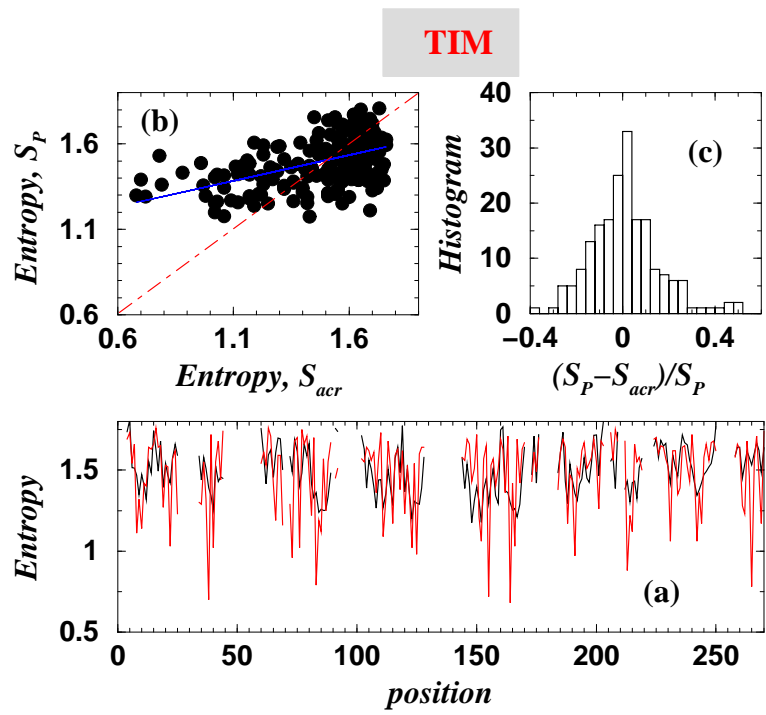


FIG. 17. (a) — (c) The same as Fig.13 but for the TIM-fold.